JOURNAL OF PROPULSION AND POWER
Vol. 25, No. 2, March–April 2009

Nanoaluminum as a Solid Propellant Fuel

Valery Babuk,* Ildar Dolotkazin,† Alexey Gamsov,‡ and Andrey Glebov§
Baltic State Technical University, 190005, St. Petersburg, Russia
and
Luigi T. DeLuca¶ and Luciano Galfetti**
Politecnico di Milano, 20156 Milan, Italy

DOI: 10.2514/1.36841

Experimental studies on the burning of nanoaluminum-based solid rocket propellants are carried out. Data on the properties of condensed combustion products, mechanisms of their formation, and burning-rate law are obtained. Based on these data, a physical picture is developed of the considered burning-propellant classes. Mathematical modeling of burning nanoaluminum in composite solid rocket propellants is carried out. The influence of nanoaluminum on ignition temperature of the metal fuel and burning-rate law is shown. The results of this study allow carrying out the analysis and selection of good-quality propellants using nanoaluminum.

Nomenclature

A, A_1, A_2, A_3	=	constant factors
a_k	=	molar fraction of oxidizing gases (oxidizing potential of the environment)
c_m	=	specific heat of the metal
c_P	=	molar isobaric specific heat
c_{PM}	=	molar isobaric specific heat of the metal vapor
D_{43}	=	mass-average diameter of agglomerates
d_{43}	=	mass-average diameter of smoke oxide particles
E, E_3	=	activation energy
$f_m\,(D)$	=	mass function of size distribution density of agglomerates
$f_m\,(d)$	=	mass function of size distribution density of smoke oxide particles
I_{sp}	=	specific impulse
$J_{\mu i}$	=	density of molar stream of the ith oxidizing gas interacting with the metal-particle surface
L_M	=	molar evaporation heat of the metal
l	=	oxide film thickness
m, m_i, m_2	=	constants
Nu	=	Nusselt number
n	=	pressure exponent
n_Σ	=	amount of oxidizing gases
P	=	pressure of the environment
P_i	=	partial pressure of ith oxidizing gas
Q_1	=	heat power released by chemical interaction of the metal with the environment
Q_2	=	heat power lost by thermal interactions of a metal particle with the environment
Q_{2c}	=	convective component of heat power
Q_{2r}	=	radiant component of heat power
Q_{2t}	=	conductive component of heat power
q_m	=	component of the heat flux value to the propellant surface caused by combustion of the metal
q_t	=	density of conductive heat flux
R	=	universal gas constant, $\text{J}/(\text{mole}\cdot\text{K})$
R_A	=	characteristic size of a particle
r_b	=	propellant steady burning rate
r_p	=	distance between metal particles
T_A	=	temperature of the metal particle
T_B	=	temperature of the burning area
T_{dc}	=	decomposition temperature of carbonaceous elements
T_{ign}	=	ignition temperature of the metal
T^*_{ign}	=	particle temperature at the moment of ignition
T_m, T	=	temperature of the metal and environment
Z_m	=	fraction of unburned metal in agglomerates relative to initial metal in propellant
Z^a_m	=	fraction of initial metal in propellant used to form agglomerates
Z^{ox}_m	=	fraction of initial metal in propellant used to form oxide in agglomerates
α	=	convective heat transfer coefficient
α_a	=	gas-phase radiation-absorption coefficient
$\Delta I_{\mu i}$	=	molar thermal effect of the interaction of the ith oxidizing gas with metal
ε	=	effective emissivity
ε_g	=	emissivity of the gas phase
ε_m	=	emissivity of the metal particles
η	=	mass fraction of oxide in agglomerate
λ	=	thermal conductivity
ρ_m	=	density of the metal
σ_0	=	Stefan–Boltzmann constant
$\varphi(\chi)$	=	parameter dependent on the particle-surface fraction free from oxide (χ)
χ	=	fraction of the metal-particle surface free from crystal oxide
Ω_1	=	area of the metal-particle surface interacting with the gas phase
Ω_2	=	area of the metal-particle surface in contact with the condensed phase
Ω_3	=	surface area of the burning metal

Received 30 January 2008; revision received 7 December 2008; accepted for publication 7 December 2008.

*Professor, Aerospace Division, Department of Space Vehicles and Rocket Motors, 1 First Krasnoarmeyskaya Street.
†Engineer, Aerospace Division, Department of Space Vehicles and Rocket Motors, 1 First Krasnoarmeyskaya Street.
‡Postgraduate Student, Aerospace Division, Department of Space Vehicles and Rocket Motors, 1 First Krasnoarmeyskaya Street.
§Assistant Professor, Aerospace Division, Department of Space Vehicles and Rocket Motors, 1 First Krasnoarmeyskaya Street.
¶Professor, Space Propulsion Laboratory, 34 Via La Masa. Associate Fellow AIAA.
**Professor, Space Propulsion Laboratory, 34 Via La Masa.

I. Introduction

ONE of the modern directions to improve solid rocket propellants is to resort to nanosized components. Within the framework of this direction, essential changes of the burning-rate law

may occur and the performance of solid propellants may increase. During the last decade, researchers of various countries undertook vigorous efforts in experimental studies regarding burning processes of nanoaluminum-based propellants. As a general rule, aluminum powders with a particle size of ~100 nm were used.

It is possible to state that the burning rates of solid rocket propellants essentially increase when changing from traditional aluminum powders into nanoaluminum [1–9]. However, the data so far collected on the influence on burning-rate magnitude and pressure sensitivity are inconsistent [1–9]. It is commonly accepted that the use of nanoaluminum causes a decrease in the metal ignition temperature [10].

Two aspects of the influence of nanoaluminum powder on propellant characteristics can be observed. First, using this ingredient yields condensed combustion products (CCP) capable of providing a decrease in specific-impulse losses. Second, using metal fuel in the form of nanostructure (i.e., particles without a volumetric phase) may result in an increase of propellant energy potential, due to the incorporation of not only chemical energy, but also intermolecular interaction energy [11]. It is emphasized that the creation of propellants based on nanostructures is now at its initial stage. In general, problems such as the creation of nanostructures and their introductions in propellant composition are not yet solved. In the open literature, one can find only a limited amount of publications (see, for example, [12]) in which similar propellants are considered.

The influence of nanoaluminum on the propellant energy characteristics is connected in particular with the influence of this ingredient on CCP characteristics. The basic process determining these characteristics is the agglomeration process.

Different interpretations exist to describe the influence of nanoaluminum on metal-fuel agglomeration at the surface layer of the burning propellant. Virtually all works ([4,13], etc.) so far carried out point out that introducing metal fuel in the form of nanoparticles implies a reduction of the CCP particle size. It is fair to say that agglomeration of burning nanoaluminum-based propellants has peculiar features that are not yet sufficiently investigated.

In addition, there is no detailed information about the characteristics of all CCP sets formed during the burning of nanoaluminum-based propellants or about the description of the CCP formation mechanism. Because this mechanism is directly connected with the influence of the metal fuel on the solid propellant burning rate, there are also problems with the description as a whole of the burning mechanism of this propellant class.

It is necessary to emphasize the rather low level of generalization of the experimental data on the burning of nanoaluminum-based solid propellants. There are open questions as to the influence of this ingredient on propellant burning rate and CCP properties. Moreover, works on mathematical modeling of nanoaluminum burning in composite solid propellants are unknown to the authors.

A significant problem regarding the fruitful use of nanoaluminum is the capability to preserve its activity. Results from recent research programs allow to look with optimism at the solution of this problem (see, for example, [14]).

The purposes of the present work are as follows:

1) Generalize the available body of experimental results regarding nanoaluminum influence on the mechanism of propellant burning.

2) Provide a mathematical model of nanoaluminum burning in the propellant surface layer.

3) Point out useful directions for effective applications of nanoaluminum.

II. Experimental Research of Burning Nanoaluminum-Based Propellants

Experimental research activities for obtaining information on the mechanism of nanoaluminum-based propellant burning have been carried out at Baltic State Technical University (St. Petersburg, Russia) and at Space Propulsion Laboratory of Politecnico di Milano (Milan, Italy).

Experiments were carried out using compositions based on inert binders and various oxidizers: ammonium perchlorate (AP), ammonium nitrate (AN), and cyclotetramethylenetetranitramine (HMX) in the pressure range of 0.1–7.0 MPa. (The data on compositions, which are quoted subsequently, are given in Tables 1 and 2 and in the text.) The experimental techniques of these investigations are described in [15–19], and their results are partly published in [20–22].

Note some basic points of the experimental methods employed: quench collection of condensed combustion products in the gas-phase zone above the burning surface and direct study of the products including mass, chemical, structural analyses, and particle size measurements; study of combustion residues obtained using special plates; measurement of propellant steady burning rate; and high-speed and high-resolution digital visualization of burning processes.

The essential features of the implemented techniques are the opportunity to collect not less than 95% of the weight of all CCP and to carry out particle analysis for sizes ranging from tens of nanometers up to 1000 μm.

The accuracy of quantitative parameters Z_m, Z_m^{ox}, Z_m^a, D_{43}, d_{43}, η, and r_b was determined by means of statistical processing of experimental data. As a rule, a high value of confidence probability (0.997) was used. Detailed information on the values of the confidence intervals is given in the cited references. Functions f_m (D) and f_m (d), described subsequently, correspond to the experiments carried out.

By analyzing the photographs of particles collected, their microsections as well as combustion residues on the plates and video recordings of burning information about the general trend of the investigated process can be obtained. Let us next consider the obtained results in a concise form.

A. Surface Layer

Investigation of the surface-layer structure was conducted by analyzing the combustion residues on inert plates [23]. It is presumed that those residues correspond to a specific structure of the surface layer, which plays a very important role in the process of propellant combustion and was given the name of the *skeleton layer* [23]. In addition, high-resolution video recording was used to analyze the surface-layer properties.

For what follows, it is convenient to review the basic features of propellant classes A and B, as already discussed in [23]. For burning propellants of class A, the metal ignition temperature is less than the decomposition temperature of carbonaceous elements. The skeleton layer of these propellants consists of a carbon skeleton with pores filled by liquid metal and oxide. For example, AN-based propellants [22] belong to class A. In contrast, for burning propellants of class B,

Table 1 AN-based composition

Substance, %	AN1	AN2
AN coarse[a]	33	33
AN fine[b]	33	33
Al regular[c]	22	——
Al nanosized[d]	——	22
Isoprene rubber	2.4	2.4
Oil ($C_{19}H_{35}$)	9	9
Additives	0.6	0.6

[a]Size of particles is 250–350 μm.
[b]Size of particles is 40–70 μm.
[c]Mass-mean diameter of particles is 10.5 μm.
[d]Specific surface is 10–20 m^2/g (size ~0.1 μm).

Table 2 (AP/HMX)-based composition

Substance, %	N2	N4
Plasticized binder	14.0	14.0
AP[a]	68.9	49.9
Al nanosized[b]	9.0	16.0
Al regular	8.0	——
HMX	——	20.0

[a]Size of particles is 160–315 μm.
[b]Specific surface 12.4 m^2/g.

the metal ignition temperature is higher than the decomposition temperature of carbonaceous elements. The skeleton layer of these propellants consists of the initial metal particles fastened among themselves. Examples of this class are propellants based on AP, inert binder, and micron-sized aluminum [23].

Based on this general distinction, it is possible to identify two types of skeleton layer for nanoaluminum-based propellants. First, it is a skeleton-layer analog of the corresponding structure of class A propellants [23]. The size of agglomerating particles forming on the surface of this layer is as close as an order of magnitude to that of the agglomerates formed for micron-sized-aluminum-based propellants. We shall designate this kind of propellant as nanoA. A distinctive feature of similar propellants based on AN is that a skeleton layer is formed in all structural formations of propellant (both in pockets and on *interpocket bridges*) [22]. In contrast, for propellants based on AP and HMX, the skeleton layer is formed only in pockets [20].

Second, it is a skeleton-layer analog of the corresponding structure of class B propellants [23]. The size of agglomerating particles on the skeleton-layer surface is smaller by more than an order of magnitude with respect to the size of agglomerates from the burning of propellants based on micron-sized aluminum. One distinctive feature of the resulting skeleton layer is that it covers the entire propellant surface free from oxidizer particles. We shall designate this kind of propellant as nanoB. The top part of the skeleton layer for a propellant type nanoB is shown in Fig. 1.

Let us emphasize the differences between propellants such as nanoA and nanoB. These differences consist of the properties of the surface layer and the size of agglomerating particles. The size for nanoA propellants is approximately 10 times that of nanoB propellants. Note that the research was carried out using only inert binders of various types. It is likely that the use of active binders will change the laws of surface-layer formation [24].

B. Condensed Combustion Products

Generally, the size of CCP particles is within rather wide bounds (from fractions of a micrometer up to 1000 μm). However, irrespective of the particle size, it is always possible to allocate two fractions that are formed by particles of two types: agglomerates and smoke oxide particles (SOP) [23,25]. Agglomerates are the particles formed by the merging of condensed substances at the propellant surface layer. Smoke oxide particles are products of metal combustion in both this layer and the layer above the propellant surface in the gas phase.

The basis for allocation of these fractions results from the analysis of mass function of particle-size distribution density. Separate modes (set of modes) correspond to the specified fractions. It is assumed that the size of agglomerates cannot be less than the size of initial metal particles.

Agglomerates, consisting of drops of aluminum and its oxide, have a fairly complex structure [20–23,26]. The present level of knowledge allows the belief that smoke oxide particles have no cavities and are of spherical form [19].

CCP properties differ essentially for propellants of the aforementioned types (nanoA and nanoB).

1. *Propellant Type NanoA*

a. Agglomerates. Formation of agglomerates occurs mainly according to the pocket mechanism [23] for propellants based on AP or HMX. The basic type of agglomerate is that with cap oxide [20]. Mass functions of agglomerate-size distribution density for one of the AP-based investigated compositions are reported in Fig. 2.

The basic types of agglomerates are hollow agglomerates for AN-based propellants [22,26]. The formation of agglomerates occurs as a result of the realization of interpocket merging. Both the mass fraction of the metal forming agglomerates ($Z_m^a \sim 0.65$) and the fraction of oxide in the composition of agglomerates ($\eta \sim 0.8$) are rather large. The mass function of agglomerate-size distribution density for one of the AN-based investigated compositions is reported in Fig. 3.

b. Smoke Oxide Particles. The size and amount of SOP essentially differ for compositions based on AP or HMX vs AN. In the first case, the size of these particles is much smaller and the amount is greater; the opposite is true in the second case. Mass functions of size distribution density of smoke oxide particles for some AP/HMX-based and AN-based investigated compositions are reported in Fig. 4.

2. *Propellant Type NanoB*

a. Agglomerates. Distinctive features of agglomerates are essentially the smaller size (Fig. 5) and increased amount ($Z_m^a \sim 0.9$). The size of agglomerates is found to be virtually independent of pressure. In addition, a new type of agglomerate is found. Agglomerates of this type are made by metal particles covered by oxide. The structure of these agglomerates is shown schematically in Fig. 6.

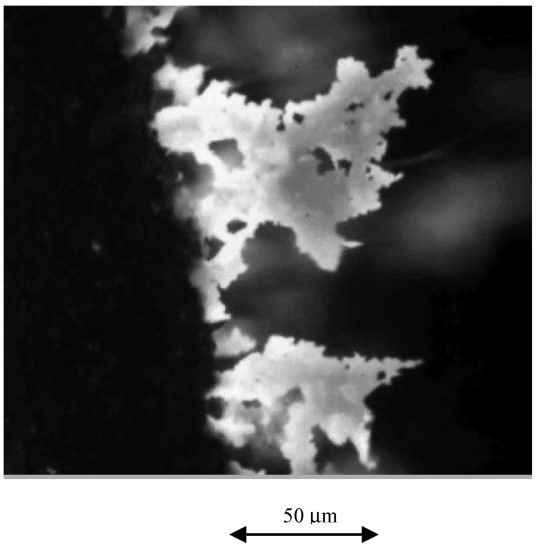

Fig. 1 Videogram fragment of the surface layer of propellant type nanoB ($P = 0.5$ MPa) based on AP/hydroxyl-terminated polybutabiene (HTPB) (courtesy of the Space Propulsion Laboratory of Politecnico di Milano).

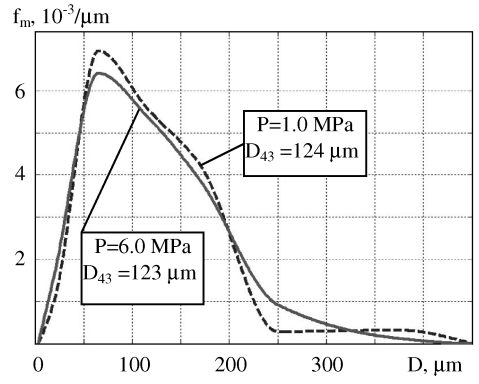

Fig. 2 Mass function of size distribution density of agglomerates for composition N2.

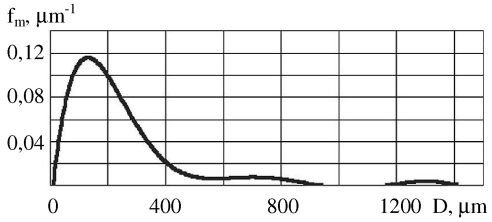

Fig. 3 Mass function of size distribution density of agglomerates for composition NA2 ($P = 6.0$ MPa).

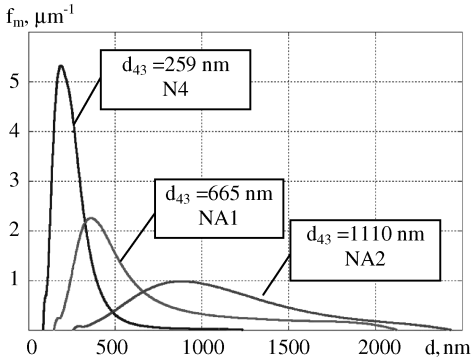

Fig. 4 Mass function of SOP-size distribution density for some compositions ($P = 6.0$ MPa).

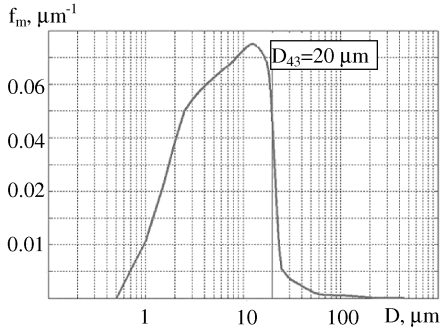

Fig. 5 Mass function of size distribution density of agglomerates for composition N4 ($P = 6.0$ MPa).

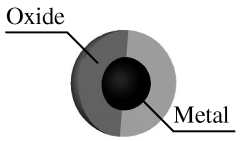

Agglomerate with
metal covered oxide

Fig. 6 Structure of agglomerates (metal covered by oxide).

b. Smoke Oxide Particles. Distinctive features of these particles are an unusually small size (Fig. 3) and a rather small amount. We shall emphasize that the fraction of these particles in a flow is determined by the value of $1 - Z_m^a$.

C. Burning Rate

Generalizing the available experimental information on burning rate of nanoaluminum-based propellants, it is possible to ascertain the following. Use of nanoaluminum unequivocally yields an increase of burning rate (Fig. 7). But the nanoaluminum's influence on the pressure exponent (n) is not unequivocal. The application of nanoaluminum can result in the increase of this parameter, its decrease, or its constancy. However, it is possible to note the following tendency. As a rule, a decrease of parameter n takes place for propellants of nanoA type, whereas the opposite is true for propellants of nanoB type.

III. Physical Picture of Burning of Nanoaluminum-Based Solid Rocket Propellants

It is to be expected that burning features of nanoaluminum-based composite solid rocket propellants are connected to the burning of the metal fuel. The behavior of this ingredient in the propellant burning wave depends on whether or not the metal fuel participates in forming the skeleton layer and on the actual skeleton-layer properties. Generally, all metal-fuel particles can be divided into two

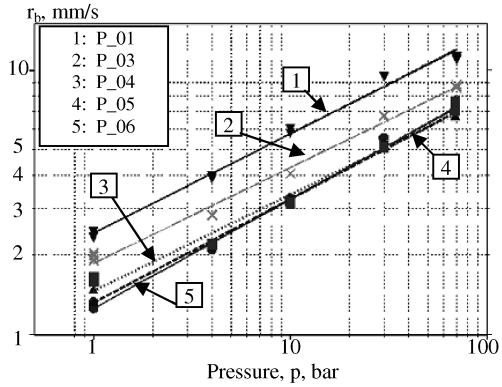

Fig. 7 Steady burning rate for some aluminized propellants: 68% bimodal AP (20% fine and 80% coarse), 15% monomodal Al, and 17% HTPB binder. (The average diameters of metal-fuel particles for compositions P_{01}–P_{06} are equal to, respectively, 0.145, 0.363, 3.035, 22.16, and 50 μm.)

groups: those forming a connected structure at the surface layer and those keeping their individuality. If agglomerates are formed only out of the metal fuel forming a skeleton layer, SOP formation generally occurs from all metal fuel. Also, burning rate generally depends on all metal fuel (i.e., whether or not it participates in the skeleton-layer formation).

Let us consider the properties of the skeleton layer for nanoaluminum-based propellants and the fraction of the metal fuel participating in the skeleton-layer formation. A necessary condition for the formation of skeleton layer is the creation of connected structures from metal particles [23]. In turn, this is connected with the occurrence of two phenomena:

1) A carbon skeleton is formed during propellant burning.

2) A connected structure is created from the initial metal particles in the propellant.

The skeleton layer for propellant type nanoA has properties similar to those of class A propellants [23]: the ignition temperature of the metal fuel is less than the decomposition temperature of carbonaceous elements (i.e., $T_{ign} < T_{dc}$). Thus, for this class of propellant, the initial metal particles lose their individuality only during agglomeration, and the initial material for formation of agglomerates is liquid Al–Al_2O_3.

The fraction of the metal fuel forming the skeleton layer depends on the ability of propellant to form a carbon skeleton. Although virtually all metal fuel participates in the skeleton-layer formation for AN-based propellants [22], only the metal fuel of pockets participates in the skeleton-layer formation for AP- and/or HMX-based propellants [20].

Smoke-oxide-particle formation occurs for agglomerating metal fuel burning in the gas-phase mode and for nonagglomerating metal fuel burning in the gas-phase layer above the surface. The size of formed particles depends on the size of burning particles, growing with an increase of the latter.

Burning of both agglomerating and nonagglomerating metal is potentially capable of affecting the propellant burning rate. An obvious condition for this effect to occur is the closeness of the metal zone with thermal emission to the propellant burning surface.

The skeleton layer for propellant type nanoB has properties similar to those of class B propellants [23]. It is assumed that the skeleton-layer formation for these propellants depends on the formation of connected structures from the initial metal particles in the propellant during its manufacture. Thus, a basic difference between propellants such as nanoA and nanoB is that the initial metal particles keep their individuality in propellants of the first type and lose it in propellants of the second type. Although not yet fully clear, we believe that the implemented manufacturing technology is the main reason for the development of propellant types nanoA and nanoB. As a matter of fact, using special pastes to introduce nanoaluminum in propellant composition promotes the occurrence of the nanoA type of propellants.

As a consequence of the formation of connected structures during the propellant manufacture, the skeleton-layer formation in this instance is not connected with the burning process. Thus, the propellant structure does not influence either the skeleton-layer formation or the fraction of the initial metal fuel participating in its formation; hence, agglomeration only depends on the degree of cohesion of the initial particles in the propellant. Experimental data give the basis to believe that this effect is rather large. Features of the skeleton-layer structure result in an increase of heat losses by metal particles during burning and therefore of their ignition temperature. Under these circumstances, the condition $T_{\text{ign}} > T_{\text{dc}}$ takes place. It represents the metal skeleton, consisting of the initial metal particles fastened among themselves. After ignition of the skeleton-layer particles, the merging and formation of agglomerating particles take place. The size and structure of formed agglomerates depend on the residence time of particles on the skeleton-layer surfaces and on the features of the agglomerating particles' evolution. The residence time is basically determined by the characteristics of the skeleton-layer nonuniformity [27]. In this instance, the occurrence of the nonuniformities responsible for agglomerating particles breaking away from the skeleton-layer surface is connected with the process of propellant manufacturing. Their characteristics do not depend on the actual burning process. This circumstance apparently determines a weak dependence of the agglomerate size on pressure.

After ignition, the burning of particles is carried out in heterogeneous mode [23]. Burning in this mode can be considered as one stage of the evolutionary process agglomerating particles on the skeleton-layer surface. Small sizes of agglomerating particles and high levels of heat losses result in a prolonged duration of this stage. A consequence of this circumstance is that the burning of some particles does not pass in gas-phase mode, and agglomerates of a new type are formed (Fig. 6), consisting of a central metal core surrounded by an oxide layer.

The formation of smoke oxide particles occurs for the combustion of only the minor portion of the initial metal that does not form connected structures. The small size of burning particles results in sharp falling of the SOP size. The burning agglomerating metal is certainly capable of influencing the propellant burning rate.

IV. Mathematical Modeling Ignition and Burning of Nanoaluminum

Mathematical modeling is meant to provide an understanding of the features of nanoaluminum burning in solid propellant compositions and their influences on the corresponding burning laws. In this respect, the ignition temperature and particle burning rate are of crucial importance. However, both phenomena are extraordinarily complex. Among the relevant factors that determine this circumstance, one should note the following:

1) Relevant fields (temperature, concentration, etc.) have a non-one-dimensional character.
2) Particles interact with the environment at high speeds.
3) Various phenomena provide this interaction.
4) There is a wide spectrum of particle sizes.

Taking the preceding into account, the possibility of exactly defining the specified properties is seen as illusory. Thus, only the influence of those or other factors on the wanted properties can be determined. First, the influence of the size of nanosized range particles was investigated.

A. Metal Ignition

The ignition temperature is one of the major characteristics of the ignition process. It is the minimum temperature at which transition to self-sustained burning is possible. The mathematical description providing a definition of this temperature is based on the energy balance equation and conditions of the failure of a thermal balance:

$$\frac{dT_m}{dt} \cdot (c_m \cdot \rho_m \cdot V_m) = \Delta Q = Q_1 - Q_2 \tag{1}$$

$$\Delta Q = Q_1 - Q_2 = 0 \qquad \frac{dQ_1}{dT} = \frac{dQ_2}{dT} \quad \text{or} \quad \frac{d(\Delta Q)}{dT} = 0 \tag{2}$$

Let us consider the situation by which the temperature of the metal particles is higher than melting temperatures but much lower than boiling temperatures. The released heat power Q_1 is generally determined as

$$Q_1 = \chi \cdot \Omega_1 \sum_{i=1}^{n_\Sigma} J_{\mu_i} \Delta I_i \tag{3}$$

where

$$J_{\mu_i} = A \cdot P_i^{m_i} \cdot \exp\left(-\frac{E}{R \cdot T}\right) \tag{4}$$

The lost heat power Q_2 includes the three components (convective, radiant, and conductive) describing the particle heat transfer with the environment:

$$Q_2 = Q_{2c} + Q_{2r} + Q_{2t} \tag{5}$$

These components can be determined as follows:

$$Q_{2c} = \alpha \cdot \Omega_1 \cdot (T_m - T) \tag{6}$$

$$Q_{2r} = \varepsilon \cdot \sigma_0 \cdot \Omega_1 \cdot (T_m^4 - T^4) \tag{7}$$

$$Q_{2t} = \Omega_2 \cdot q_t \tag{8}$$

The solution of the system of equations (1) and (2) in view of expressions (3–8) allows us to determine the temperature values T and T_m, which provide an estimate of the ignition temperature T_{ign} and particle temperature at the moment of ignition (T^*_{ign}).

Let us consider the principles of determination of values Q_1 and Q_2 under various conditions. The laws of chemical kinetics interaction of the metal with the gas phase are different for pockets and interpocket bridges. In the first case, one can assume that the rate of chemical interaction is determined by the diffusion of oxidizing components in the gas phase. Then Eq. (4) takes the following form:

$$J_\mu = A_1 \cdot a_k \cdot \exp\left(-\frac{E}{R \cdot T}\right) \tag{9}$$

In the second case, considering the gas-phase properties for interpocket bridges [23,28], one can assume that the rate of the interaction is determined by processes of adsorption (desorption) and the actual chemical interaction between the metal and gas dissolved in it. The basic oxidizing gases are CO_2 and H_2O. Taking into account that these gases are triatomic, their dissociation is rather probable at adsorption.

Taking into account the nature of the phenomena determining the chemical interaction rate, a possible range of values for the parameter m in Eq. (4) is 0–1. By accepting $m = 0.5$, the kinetic interaction is described as

$$J_\mu = A_2 \cdot a_k^{0.5} \cdot P^{0.5} \exp\left(-\frac{E}{R \cdot T_m}\right) \tag{10}$$

The greatest interest is represented by the radiant component of the heat flux when estimating the Q_2 value. This depends on the distance r_p between metal particles. The resulting emissivity is a function of this distance [i.e., $\varepsilon = \varepsilon(r_p)$]. It is possible to estimate the value of ε as follows:

$$\varepsilon = \varepsilon_m \cdot \varepsilon_g \tag{11}$$

with

$$\varepsilon_g = 1 - \exp(-\alpha_a \cdot r_p)$$

where α_a is the gas-phase radiation-absorption coefficient. The dependence of the parameter r_p on the amount of particles, and hence their size, is obvious. When the size of particles is reduced, heat losses fall and the ignition temperature drops as well.

Let us consider some results of numerical simulations. Reducing the size of the metal initial particles unequivocally yields a drop of ignition temperature (Fig. 8). This result holds true for both pockets and interpocket bridges. However, for increasing pressures, the value of T_{ign} varies insignificantly for pockets, whereas it falls for interpocket bridges. This result is due to the fact that the chemical interaction rate does not depend on pressure for pockets, whereas it increases with increasing pressure for interpocket bridges [Eqs. (9) and (10)].

It is of interest to compare the T_{ign} values in the skeleton layer of propellant types nanoA and nanoB. The skeleton-layer features for the nanoB propellant type result in larger conductive heat losses by particles and, as a consequence, in larger T_{ign} values.

The results of modeling show that if the initial nanoaluminum particles in propellant keep their individuality, the metal ignition temperature falls. Otherwise, in propellants with connected structures, this temperature increases.

B. Metal Burning

It is possible to assume that the physical nature of burning nanosized aluminum does not undergo significant changes and that its burning law is the same as that of micron-sized aluminum. If so, differences would consist only of a sharp increase in the particle burning surface. However, interesting work has recently been conducted for nanoaluminum particles burning in a shock tube, showing a transition from vapor-phase diffusion-limited to near-surface-limited combustion (Bazyn et al. [29,30]).

The burning of metal fuel in a surface layer is a multistage process [9,23]. Burning is carried out in a heterogeneous mode directly after ignition. At the first stage, the gaseous oxidizer interacts with the metal for which mechanical destruction of the initial oxide film occurs. The oxide so formed does not provide restoration of the oxide film's protective properties. The kinetic processes are determined by the oxidizing component's diffusion in the gas phase for metal-fuel pocket burning or by oxidizing-gas adsorption for metal-fuel interpocket-bridge burning. The second stage begins when the particle temperature reaches the oxide melting point, when particles become covered by a continuous fused-oxide film. The burning kinetics at this stage are determined by the diffusion of reacting components through this film. The second stage ends after the break of the oxide film and transition of burning to the gas-phase mode. The time dependence of the particle temperature after ignition is schematically shown in Fig. 9.

Equations (9) and (10) can be used to describe the particle burning kinetics at the first stage of heterogeneous burning for the conditions of pocket and interpocket bridges. For the second stage of heterogeneous burning, the kinetics are described by the following expression [9,28]:

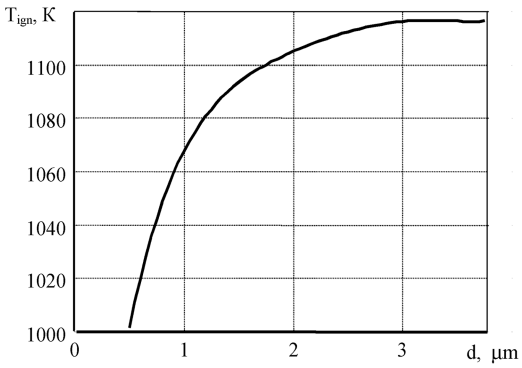

Fig. 8 Dependence of the temperature of metal ignition on the size of particles ($P = 4.0$ MPa).

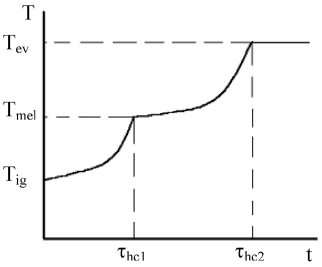

Fig. 9 Dependence of the temperature of a burning particle on time (t_{hc1} and t_{hc2} are the moments of time corresponding to the end of the first and the second stage of heterogeneous combustion).

$$J_{\mu 3} = \frac{A_3}{l} \cdot \exp\left(-\frac{E_3}{R \cdot T_m}\right) \cdot T_m \cdot a_k^{m_2} \tag{12}$$

where $J_{\mu 3}$ is the molar stream density of a substance at the second stage of heterogeneous burning, and $m_2 \sim 1.5$–2.0.

For the description of the gas-phase burning kinetics, the expressions obtained for the agglomerates' evolution in the gas phase [31] can be used:

$$J_{\mu 4} = \frac{A_4 R_A \varphi(\chi) Nu}{\Omega_3} \cdot \left(\frac{\lambda}{c_p}\right)_{\text{I}} \cdot \left\{\frac{2}{3} a_k + \left(\frac{c_p}{\lambda}\right)_{\text{I}} \cdot \left(\frac{\lambda}{c_p}\right)_{\text{II}} \cdot \ell_n\left(\frac{c_{p_M}(T_B - T_A)}{L_M} + 1\right)\right\} \tag{13}$$

where $J_{\mu 4}$ is the molar stream density of a substance at the gas-phase burning stage, I is the area between the particle surface and the burning zone, and II is the area between the burning zone and the environment.

C. Metal Burning and Burning Rate of Propellant

A model describing the metal burning influence on the propellant burning rate was proposed in [32]. Thismodel is based on the Beckstead–Derr–Price philosophy [33]. Results of numerical simulation obtained through this model have shown a nano-aluminum influence on the propellant burning rate, which involves a reduction of the T_{ign} value.

For propellant type nanoA, if the metal-fuel combustion is basically carried out at the boundaries of pockets, a decrease in burning-rate dependence on pressure takes place. Otherwise, if a significant fraction of the interpocket bridges exists, this dependence grows. This growth is a consequence of the fact that when metal fuel burns at the pocket boundaries, the basic contribution to the heat flux to the propellant surface, due to metal combustion q_m, causes metal burning according to the first stage of heterogeneous burning. This is carried out in diffusive mode. As a result, a decrease in the pressure dependence of the heat flux acting on the propellant condensed phase takes place for increasing pocket fraction.

For propellant type nanoB, the skeleton-layer features an increased heat conductivity. This causes an increase of q_m at the second stage of heterogeneous metal-fuel burning. The dependence of the heat intensity on pressure at this stage has a contradictory character. On one hand, by increasing the pressure, the thickness of the oxide layer [parameter l in Eq. (12)] increases, and therefore the burning rate decreases. On the other hand, the particle temperature increases, accelerating the diffusion rate of reacting components in liquid oxide and the metal burning rate. However, as the dependence of the diffusion rate on temperature has an exponential character, the second factor prevails. Then with an increase in pressure, the heat intensity as a whole increases. Thus, the metal-fuel influence on the burning rate of propellant type nanoB results in some increase of the pressure exponent.

V. Conditions for Effective Use of Nanoaluminum

Let us consider the requirements for the use of nanoaluminum as a fuel in solid rocket propellants. Under the condition of preserving a

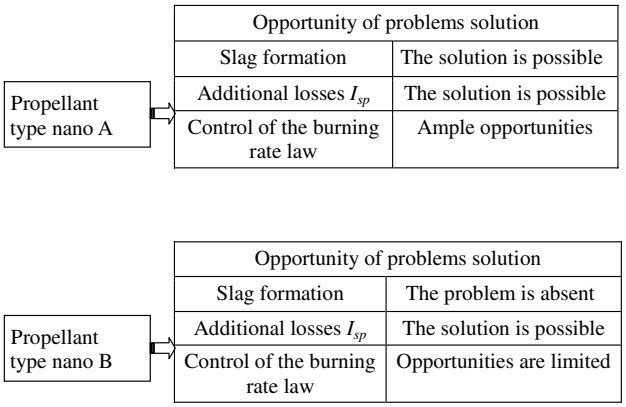

Fig. 10 Type and behavior of propellants based on nanosized aluminum.

fairly high reactivity of the metal fuel, the requirements can be formulated as follows:

1) There is an increase in burning rate and decrease in its pressure dependence.

2) There is a search of the agglomeration process parameters, leading to insignificant slag formation in the motor chamber.

3) There is a minimization of losses of specific impulse I_{sp}.

The results obtained in this paper allow a number of conclusions concerning the efficient use of nanoaluminum as a solid rocket propellant fuel. As for the choice of types nanoA and nanoB, further investigations are necessary. In the case of propellants of type nanoB, the problem of slag formation in the motor chamber is virtually absent. However, the possibility of metal agglomerates being covered by oxide can result in an increase of combustion inefficiency and specific-impulse losses. In the case of propellants of type nanoA, one can imagine an ideal situation in which the ratio between the two basic CCP fractions is optimum, leading to minimum slag formation and minimum I_{sp} losses. In addition, for propellants of this type, a higher metal-fuel influence on the propellant burning rate is typically observed, which results in a pressure exponent reduction. These ideas are illustrated in the scheme of Fig. 10.

VI. Conclusions

The research carried out allowed the following basic results to be obtained:

1) Laws of the surface-layer formation, condensed products combustion, and burning rate of nanoaluminum-based propellants were experimentally established.

2) The general physical picture of the burning of nanoaluminum-based propellants was developed.

3) The mathematical description of the ignition and burning of metal fuel in the propellant surface layer was developed. The character of nanoaluminum influence on the propellant burning rate was shown.

4) Consequences of using nanoaluminum on the propellant behavior were determined.

Directions of future works, in our opinion, should be focused on studying propellant burning with nanoparticles in a size range of less than 50–100 nm (i.e., particles coming closer to the properties of nanostructures). Of course, reducing the size of particles makes it increasingly difficult to preserve the quantity of active metal until the use of nanoaluminum as a propellant component falls.

Acknowledgments

This work was carried out with the support of the Russian Foundation for Basic Research (project 08-08-00118-a). The authors wish to thank the careful and diligent work of the many students who actually performed the experimental work in the laboratories of the Space Vehicles and Rocket Motors Department at Baltic State Technical University, St. Petersburg, and the SPLab (Space Propulsion Laboratory) at Politecnico di Milano. Thanks are due to Filippo Maggi for providing helpful high-resolution images. Special thanks are due to Woodward Waesche and Hugh McSpadden for useful discussions.

References

[1] Armstrong, R. W., Kramer, M. P., and Wilson, W. H., "The Power and Strength of Energetic/Reactive Nano-Materials," *9th International Workshop on Combustion and Propulsion (9-IWCP)*, Lerici, La Spezia, Italy, Sept. 2003, pp. 56–57.

[2] Mench, M. M., Yeh, C. L., and Kuo, K. K., "Propellant Burning Rate Enhancement and Thermal Behavior of Ultra-Fine Aluminum Powders (ALEX)," 29th International Annual Conference of ICT, Inst. Chemische Technologie Paper 30, 1998.

[3] Lessard, P., Beaupre, F., and Brousseau, P., "Burn Rate Studies of Composite Propellants Containing Ultra-Fine Metals," *Proceedings of the 32nd International Annual Conference of ICT*, Inst. Chemische Technologie Paper 88, July 2001.

[4] Dokhan, A., Price, E. W., Sigman, R. K., and Seitzman, J. M., "The Effects of Al Particle Size on the Burning Rate and Residual Oxide in Aluminized Propellants," 37th AIAA/ASME/ASEE Joint Propulsion Conference and Exhibit, Salt Lake City, UT, 2001, AIAA Paper 01-3581.

[5] Vorozhsov, A. B., Arkhipov, V., Bondarchuk, S., Korotkikh, A., Kuznezov, V., Surkov, V., and Sedoi, V., "Ignition and Combustion of Solid and Gelled Propellants Containing Ultra-Fine Aluminum," *Rocket Propulsion: Present and Future, Proceedings of the Eighth International Workshop on Combustion and Propulsion (8-IWCP)*, edited by L. T. DeLuca, Grafiche GSS, Bergamo, Italy, 2003, Paper 36.

[6] Arkhipov, V. A., Korotkikh, A. G., and Kuznezov, V. T., "Ignition and Combustion of Condensed Systems Containing Ultra-Fine Aluminum," *Fundamental and Applied Problems of Modern Mechanics*, Tomsk State Univ., Tomsk, Russia, 2002, pp. 28–29 (in Russian).

[7] Arkhipov, V. A., Ivanov, G. V., Korotkikh, A. G., Medvedev, V. V., and Surkov, V. G., "Features of Ignition and Burning Composition Propellants with Utra-Fine Aluminum (ALEX)," *Proceedings of the International Seminar on Intra-Chamber Processes, Combustion and Gas Dynamics of Dispersed Systems*, Baltic State Technical Univ., St. Petersburg, Russia, 2000, pp. 80–81 (in Russian).

[8] Baschung, B., Grune, D., Licht, H. H., and Samirant, M., "Combustion Phenomena of a Solid Propellant Based on Aluminum Powder," *Combustion of Energetic Materials*, edited by K. Kuo, and L. T. DeLuca, Begell House, New York, 2002, pp. 219–223.

[9] Babuk, V. A., Vasilyev, V. A., Dolotkazin, I. N., and Sviridov, V. V., "Metal Fuel as Component of High-Performance Solid Rocket Propellants: Problems and Applications Perspective," *Rocket Propulsion: Present and Future, Proceedings of the Eighth International Workshop on Combustion and Propulsion (8-IWCP)*, edited by L. T. DeLuca, Grafiche GSS, Bergamo, Italy, 2003, Paper 26.

[10] Son, S. F., Yetter, R. A., and Yang, V., "Introduction: Nanoscale Composite Energetic Materials," *Journal of Propulsion and Power*, Vol. 23, No. 4, 2007, pp. 643–644. doi:10.2514/1.31508

[11] Babuk, V. A., "Nanostructures, as New Object of Study of the Nature World. Properties, Condition of Application and Obtaining," *Proceedings of International Workshop on MEMS and Nanotechnology Integration (MNI): Applications*, Inst. of Electrophysics, Russian Academy of Sciences, Ekaterinburg, Russia, 2004, p. 82.

[12] Ramaswamy, A. L., Kaste, P., and Trevino, S., "Nano-Scale ingredients for Environmentally Benign Propellants," *Rocket Propulsion: Present and Future, Proceedings of the Eighth International Workshop on Combustion and Propulsion (8-IWCP)*, edited by L. T. DeLuca, Grafiche GSS, Bergamo, Italy, 2003, Paper 35.

[13] Glotov, O. G., Zarko, V. E., and Beckstead, M. W., "Agglomerated and Oxide Particle Generated in Combustion of ALEX Containing Solid Propellants," 31st International Annual Conference of ICT, Inst. Chemische Technologie Paper 130, June 2000.

[14] Dubois, C., Lafleur, P. G., and Roy, C., "Polymer Grafted Metal Nanoparticles for Fuel Applications," *Journal of Propulsion and Power*, Vol. 23, No. 4, 2007, pp. 651–658. doi:10.2514/1.25384

[15] Babuk, V. A., Vasilyev, V. A., and Malakhov, M. S., "Condensed Combustion Products at the Burning Surface of Aluminized Solid Propellant," *Journal of Propulsion and Power*, Vol. 15, No. 6, 1999, pp. 783–794. doi:10.2514/2.5497

[16] Galfetti, L., Severini, F., DeLuca, L. T., Marra, G., and Braglia, R.,

"Ballistics and Condensed Combustion Residues of Aluminized Solid Rocket Propellants," *Novel Energetic Materials and Applications, Proceedings of the Ninth International Workshop on Combustion and Propulsion (9-IWCP)*, edited by L. T. DeLuca, L. Galfetti, and R. A. Pesce-Rodriguez, Grafiche GSS, Bergamo, Italy, 2004, Paper 18.

[17] DeLuca, L. T., Galfetti, L., Severini, F., Galeotta, M., DeAmicis, R., Babuk, V. A., Kondrikov, B. N., and Vorozhtsov, A. B., "Solid Rocket Motors for Cheap Access to Space," *Novel Energetic Materials and Application, the Ninth International Workshop on Combustion and Propulsion (9-IWCP)* [CD-ROM], Lerici, La Spezia, Italy, Sept. 2003.

[18] Taiariol, P., Galeotta, M., and DeLuca, L. T., "Burning Waves Visualization with Digital High Speed Color Camera," *Novel Energetic Materials and Application, Ninth International Workshop on Combustion and Propulsion (9-IWCP)* [CD-ROM], Lerici, La Spezia, Italy, Sept. 2003.

[19] Babuk, V. A., "Problems in Studying Formation of Smoke Oxide Particles in Combustion of Aluminized Solid Propellants," *Combustion, Explosion, and Shock Waves*, Vol. 43, No. 1, 2007, pp. 38–45. doi:10.1007/s10573-007-0006-5

[20] Babuk, V. A., Glebov, A., Dolotkazin, I., Conti, A., Galfetti, L., DeLuca, L. T., and Vorozhtsov, A., "Condensed Combustion Products from Burning of Nanoaluminum-Based Propellants: Properties and Formation Mechanism," *Advances in Aerospace Sciences*, Torus Press (to be published).

[21] DeLuca, L. T., Galfetti, L., Severini, F., Meda, L., Marra, G., Vorozhtsov, A. B., Sedoi, V. S., and Babuk, V. A., "Burning of Nano-Aluminized Composite Rocket Propellants," *Combustion, Explosion, and Shock Waves*, Vol. 41, No. 6, 2005, pp. 680–692. doi:10.1007/s10573-005-0080-5

[22] Babuk, V. A., Vasilyev, V. A., Glebov, A. A., Dolotkazin, I. N., Galeotta, M., and DeLuca, L. T., "Combustion Mechanisms of AN-Based Aluminized Solid Rocket Propellants," *Novel Energetic Materials and Applications, Proceedings of the Ninth International Workshop on Combustion and Propulsion (9-IWCP)*, edited by L. T. DeLuca, L. Galfetti, and R. A. Pesce-Rodriguez, Grafiche GSS, Bergamo, Italy, 2004, Paper 44.

[23] Babuk, V. A., Vasilyev, V. A., and Sviridov, V. V., "Formation of Condensed Combustion Products at the Burning Surface of Solid Rocket Propellant," *Solid Propellant Chemistry, Combustion, and Motor Interior Ballistics*, edited by V. Yang, T. B. Brill, and W. Z. Ren, Progress in Astronautics and Aeronautics, AIAA, Reston, VA, 2000, pp. 749–776.

[24] Babuk, V. A., Glebov, A. A., and Dolotkazin, I. N., "Burning Mechanism of Aluminized Solid Rocket Propellants Based on Energetic Binders," *Propellants, Explosives, Pyrotechnics*, Vol. 30, No. 4, 2005, pp. 281–290. doi:10.1002/prep.200500012

[25] Price, E. W., and Sigman, R. K., "Formation of Condensed Combustion Products at the Burning Surface of Solid Rocket Propellant," *Solid Propellant Chemistry, Combustion, and Motor Interior Ballistics*, edited by V. Yang, T. B. Brill, and W. Z. Ren, Progress in Astronautics and Aeronautics, AIAA, Reston, VA, 2000, pp. 749–776.

[26] Babuk, V. A., Glebov, A., Arkhipov, V. A., Vorozhtsov, A. B., Klyakin, G. F., Severini, F., Galfetti, L., and DeLuca, L. T., "Dual-Oxidizer Solid Rocket Propellants for Low-Cost Access to Space," *In-Space Propulsion, Proceedings of the Tenth International Workshop on Combustion and Propulsion (10-IWCP)*, edited by L. T. DeLuca, R. L. Sackheim, B. A. Palaszewski, Grafiche GSS, Bergamo, Italy, Nov. 2005, Paper 15.

[27] Babuk, V. A., Dolotkazin, I. N., and Sviridov, V. V., "Simulation of Agglomerate Dispersion in Combustion of Aluminized Solid Propellants," *Combustion, Explosion, and Shock Waves*, Vol. 39, No. 2, 2003, pp. 195–203. doi:10.1023/A:1022917201681

[28] Babuk, V. A., "Combustion of Metal Fuel in Surface Layer of Solid Rocket Propellant," *Intra-Chamber Processes, Combustion and Gas Dynamics of Dispersed Systems*, Vol. 1, Baltic State Technical Univ., St. Petersburg, Russia, 1997, pp. 194–219 (in Russian).

[29] Bazyn, T., Krier, H., and Glumac, N., "Combustion of Nanoaluminum at Elevated Pressure and Temperature behind Reflected Shock Waves," *Combustion and Flame*, Vol. 145, No. 4, 2006, pp. 703–713. doi:10.1016/j.combustflame.2005.12.017

[30] Bazyn, T., Krier, H., and Glumac, N., "Evidence for the Transition from the Diffusion-limit in Aluminum Particle Combustion," *Proceedings of the Combustion Institute*, Vol. 31, No. 2, 2007, pp. 2021–2028. doi:10.1016/j.proci.2006.07.161

[31] Babuk, V. A., and Vasilyev, V. A., "Model of Aluminum Agglomerate Evolution in Combustion Products of Solid Rocket Propellant," *Journal of Propulsion and Power*, Vol. 18, No. 4, 2002, pp. 814–824. doi:10.2514/2.6005

[32] Babuk, V. A., Gamzov, A. V., Glebov, A. A., Dolotkazin, I. N., and Dosychev, A. V., "Structure of Composite Metallized Solid Propellants and Its Role During Burning," *Khimicheskaya Fizika i Mesoskopiya*, Vol. 8, No. 1, 2006, pp. 33–45 (in Russian).

[33] Cohen, N. S., "Review of Composite Propellant Burn Modeling," *Journal of Propulsion and Power*, Vol. 18, No. 3, 1980, pp. 277–293.

S. Son
Associate Editor